J. Pharm. Pharmacol. 1998, 50: 989–996
Received October 16, 1997
Accepted May 19, 1998

Pharmacokinetics and Tissue Distribution of (±)-3′-Azido-2′,3′-dideoxy-5′-*O*-(2-bromomyristoyl)thymidine, a Prodrug of 3′-Azido-2′,3′-dideoxythymidine (AZT) in Mice

KEYKAVOUS PARANG, LEONARD I. WIEBE* AND EDWARD E. KNAUS

Faculty of Pharmacy and Pharmaceutical Sciences, University of Alberta, Edmonton, Alberta, Canada T6G 2N8

Abstract

The in-vivo biodistribution and pharmacokinetics in mice of 3′-azido-2′,3′-dideoxythymidine (**1**, AZT), 2-bromomyristic acid (**2**) and their common prodrug, (±)-3′-azido-2′,3′-dideoxy-5′-*O*-(2-bromomyristoyl)thymidine (**3**) are reported. The objectives of the work were to enhance the anti-human immunodeficiency virus and anti-fungal effects of **1** and **2** by improving their delivery to the brain and liver.

The pharmacokinetics of AZT ($\beta t_{1/2}$ (elimination, or beta-phase, half-life) = 112·5 min; AUC (area under the plot of concentration against time) = 29·1 ± 2·9 μmol g^{-1} min; CL (blood clearance) = 10·5 ± 1·1 mL min^{-1} kg^{-1}) and its ester prodrug (**3**, $\beta t_{1/2}$ = 428·5 min; AUC = 17·3 ± 4·7 μmol g^{-1} min; CL = 17·6 ± 4·8 mL min^{-1} kg^{-1}) were compared after intravenous injection of equimolar doses (0·3 mmol kg^{-1}) via the tail vein of Balb/c mice (25–30 g). The prodrug was rapidly converted to AZT in-vivo, but plasma levels of AZT (peak concentration 0·17 μmol g^{-1}) and AUC (12·3 μmol min g^{-1}) were lower than observed after AZT administration (peak concentration 0·36 μmol g^{-1}; AUC 29·1 μmol min g^{-1}). The prodrug also accumulated rapidly in the liver immediately after injection, resulting in higher concentrations of AZT than observed after administration of AZT itself (respective peak concentrations 1·11 and 0·81 μmol g^{-1}; respective AUCs 42·5 and 12·7 μmol min g^{-1}). Compared with doses of AZT itself, **3** also led to significantly higher brain concentration of AZT (25·7 compared with 9·8 nmol g^{-1}) and AUCs (2·8 compared with 1·4 μmol min g^{-1}). At the doses used in this study the antifungal agent 2-bromomyristic acid was measurable in plasma and brain within only 2 min of injection. Hepatic concentrations of 2-bromomyristic acid were higher for at least 2 h after dosing with **3** than after dosing with the acid itself.

In summary, comparative biodistribution studies of AZT and its prodrug showed that the prodrug led to higher concentrations of AZT in the brain and liver. Although the prodrug did not result in measurably different concentrations of 2-bromomyristic acid in the blood and brain, it did lead to levels in the liver which were higher than those achieved by dosing with the acid itself.

Human immunodeficiency virus (HIV) invades the central nervous system (CNS), culminating in severe neurological disorders (Koenig et al 1986). Because 3′-azido-2′,3′-dideoxythymidine (AZT, **1**) is a poor permeant of the blood–brain barrier, it does not effectively suppress viral replication in the brain. Theoretically this could be resolved simply by administering larger doses, but this is limited by the dose-related bone-marrow toxicity of AZT. It has also been shown that bulk efflux of AZT from the brain via the organic-anion-transport system has an important effect on AZT levels attainable (Wang & Sawchuk 1995).

A variety of infections of the CNS, including, most importantly, *Cryptococcus neoformans* infections, also complicate late-stage HIV-1 infection. *Cryptococcal meningitis* is the most common CNS fungal infection in AIDS, eventually affecting 5–10% of patients (Diamond 1995). Several (±)-2-halotetradecanoic acids, including (±)-2-bromotetradecanoic acid (2-bromomyristic acid, **2**),

Correspondence: L. I. Wiebe, Faculty of Pharmacy and Pharmaceutical Sciences, 3118 Dentistry–Pharmacy Building, University of Alberta, Edmonton, Alberta, Canada T6G 2N8.

are active against *C. neoformans* (minimum inhibitory concentration, MIC, $= 20\,\mu M$) in RPMI 1640 medium (Parang et al 1996) and might be suitable for the treatment of cryptococcal meningitis in AIDS patients.

Many investigators have exploited the relationship between brain-capillary permeability and the *n*-octanol–water partition coefficients of permeants (Levin 1980) to design agents which can cross the blood–brain barrier more readily. Fatty acid esterification of the 5′-hydroxyl group of anti-HIV nucleosides has been used to produce prodrugs that have higher partition coefficients (7·2–17·9) and increased cellular uptake (up to fourfold higher) compared with AZT (Aggarwal et al 1990; Kawaguchi et al 1990). Although in-vitro and in-vivo evaluations of ester prodrugs have shown improved site-specific delivery or pharmacokinetic parameters, or both, for the parent nucleoside, these modifications have not produced clear-cut improvements in therapeutic efficacy. Prodrugs which have a longer residence time in the body and provide sustained release of the parent drug at concentrations adequate for therapeutic anti-HIV efficacy, but not causing toxicity, are still needed (Pizzo 1990). The utility of 5′-fatty acyl-AZTs as potential prodrugs of AZT is dependent upon their pharmacokinetic properties, tissue distribution and rate of bioconversion to AZT. The pharmacokinetic disposition of AZT in mice has been described elsewhere (Doshi et al 1989; Chu et al 1990; Kawaguchi et al 1990; Namane et al 1992).

The dual acting prodrug (±)-3′-azido-2′,3′-dideoxy-5′-*O*-(2-bromomyristoyl)thymidine (**3**) was designed to improve the delivery of both AZT (**1**) and the anti-fungal myristic acid analogue (**2**) to the CNS. The slow conversion of **3** to **1** and **2** in the blood, and its enhanced lipophilicity (log P = 8·14), suggest that **3** might furnish higher concentrations of the active drugs (**1** and **2**) in the brain and might also deliver a larger percentage of the dose to macrophages and other HIV-infected cells (Figure 1).

The pharmacokinetics of AZT (**1**) and (±)-3′-azido-2′,3′-dideoxy-5′-*O*-(2-bromomyristoyl)thymidine (**3**), and the concentrations of **1**, **2** and **3** in the brain and liver of male Balb/c mice are now reported.

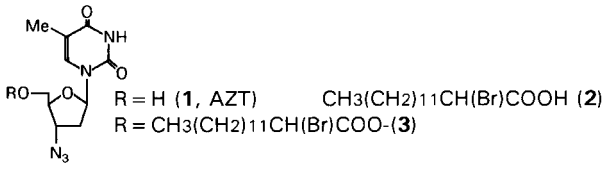

Figure 1. Structures of AZT (**1**), 2-bromomyristic acid (**2**) and their common prodrug (±)-3′-azido-2′,3′-dideoxy-5′-*O*-(2-bromomyristoyl)thymidine (**3**).

Materials and Methods

Chemicals

3′-Azido-2′,3′-deoxythymidine (AZT, **1**) was prepared by means of a procedure reported in the literature (Czernecki & Valery 1991). An improved and convenient one-pot synthesis of esters (Kamijo et al 1984), using 1,1′-carbonyldiimidazole in the presence of a reactive halide, was used for the synthesis of the 2-bromomyristoyl (**3**, 44%) ester of **1**. Thus, 1,1′-carbonyldiimidazole was treated with methyl iodide (2 eq) in acetonitrile, and then **2** (1 eq) was added to the solution followed by addition of **1** to afford the prodrug ester (**3**).

Animals

Male Balb/c mice, 25–30 g, were purchased from the University of Alberta Health Sciences Laboratory Animal Services Facility. The biotransformation and pharmacokinetic parameters for all three compounds were investigated in mice at equimolar doses (0·31 mmol kg^{-1}; **3**, 169·8 mg kg^{-1}; **1**, 81·5 mg kg^{-1}; **2**, 93·7 mg kg^{-1}), administered intravenously via the dorsal tail-vein over 30 s. **1** and **2** were administered simultaneously in the same solution to one group of mice and the prodrug (**3**) was administered to a second group. All three test compounds were dissolved in polyethylene glycol (PEG) 200–ethanol (70 : 30, v/v). Animals were killed by carbon dioxide asphyxiation 1, 2, 4, 8, 16, 32, 64, 128, 256, 512, 1440 min after dosing, and blood, liver and brain specimens were collected immediately and quickly (within 90 s of death) frozen on dry ice. At least three mice were used for each time-point.

Analysis of blood, liver and brain samples

Distilled water (100 μL) and 5-bromo-2′-deoxyuridine (100 μL; 5 mg mL^{-1} in water, internal standard) were added to blood specimens (200 μL) and vortex mixed. Acetonitrile–DMSO (800 μL, 92 : 8, v/v) was added to the mixture which was then centrifuged (30 min; 1500 *g*). The supernatant was collected and stored frozen at −22°C in the dark before quantitative analysis by high-performance liquid-chromatography (HPLC). The supernatant solution was also analysed by HPLC (20 μL injection).

Distilled water (300 μL) and internal standard solution (300 μL; 5 mg mL^{-1} in water) were added to the weighed solid tissues (brain and liver) and the mixtures were homogenized (5 min) in

acetonitrile–DMSO (92 : 8, v/v); the ratio of tissue homogenate to mixed organic solvent was 1 : 2 w/v. The homogenate was centrifuged (1500 *g*; 15 min) and the supernatant was analysed by HPLC (20 μL injection). All experiments were performed in triplicate.

A similar procedure, using different amounts of standard solutions (100 μL for blood, 300 μL for liver and brain), was used to prepare HPLC calibration curves in which the ratio of the peak areas for the different concentrations of standard solutions of **1**, **2** and **3** were plotted as functions of the area of the internal standard peak. Calibration curves were calculated by least-square regression analysis. The sample AUC (area under the plot of concentration against time) ratios AZT/internal standard, 2-bromomyristic acid/internal standard and ester/internal standard were used to calculate concentrations from the linear regression equation for the respective standard.

Quantitative and qualitative analysis of samples were performed by HPLC with Waters baseline 810 software operating on a 486/33 MHz computer. A Waters model 501 pump, Waters model U6K injector, Hewlett-Packard 1040A photodiode-array detector or Waters 486 variable wavelength detector (265 nm), and a HP 79994A workstation or a Waters system interface module, were used for analysis of **1** and **3**. An evaporative light-scattering detector (Varex MK III, Alltech) was used to detect and quantify **2**.

Several HPLC conditions were developed for the analysis of these compounds. Samples from the in-vivo studies of **1** and **3** were analysed on a Phenomenex 250 mm × 4·60 mm × 5 μm particle size Partisil 5 ODS(3) column; a complex gradient of acetonitrile and water was used as mobile phase. Details of the separation are shown in Table 1. The retention times for 5-bromo-2′-deoxyuridine (internal standard), **1** and **3** were 12·3, 22·3 and 49·9 min, respectively. The identity of each compound present in the sample was determined by comparing its retention time with that of an authentic sample. The quantification limit for each compound was based on a signal-to-noise ratio of 3 : 1. When this criterion was applied the sensitivity limits in blood for **1** and **3** were 0·4 and 1·8 ng g^{-1}, respectively.

HPLC analysis of 2-bromotetradecanoic acid (**2**) was performed on an 8 mm i.d. × 10 cm length × 10 μm particle size Waters Radial-Pak C_{18} reversed-phase cartridge column; an acetonitrile–water gradient was used as mobile phase (flow rate 1 mL min^{-1}). The light-scattering detector was operated at a drift-tube temperature of 100 ± 0·2°C, with gas flow at 3·12 standard L min^{-1} and a solvent (gauge) pressure of 7·2–7·4 pounds per square inch. Retention times for **1**, 5-bromo-2′-deoxyuridine and **2** were 3·3, 4·5 and 27 min, respectively (Table 2).

Data analysis

The pharmacokinetic parameters for **1**, but not **2**, were determined after intravenous administration of **1** and **3**. The area under the plot of concentration against time (AUC) for blood, brain and liver was calculated by computer running WinNonlin version 1.0 (Scientific Consulting). WinNonlin uses the linear trapezoidal method to calculate the AUC from time zero to the time of the last sample (AUC_{last}), which then is extrapolated to infinity. Data are reported as means ± standard errors unless stated otherwise. Blood levels for AZT (**1**) after administration of **1** or **3** declined in a biphasic manner which was best described by a two-compartment pharmacokinetic model, $C_t = Ae^{\alpha t} + Be^{\beta t}$, where C_t is the concentration at time t, A is the distribution phase intercept, α is the distribution phase slope, B is the elimination phase intercept, β is the elimination phase slope, e is the natural logarithm base, and t is time after injection. Adequacy of model fit was judged by the residual sums of squared deviations and the correlation between observed and predicted blood drug levels. The terminal disposition rate-constant (λz) was equal to the slope of the equation obtained from linear

Table 1. Mobile-phase gradient used for HPLC analysis of 3′-azido-2′,3′-dideoxythymidine and (±)-3′-azido-2′,3′-dideoxy-5′-*O*-(2-bromomyristoyl)thymidine in biological samples.

Time (min)	Amount of acetonitrile (%)	Amount of water (%)
0	5	95
17	20	80
19	60	40
22–35	70	30
40–70	90	10
85	5	95

Table 2. Mobile-phase gradient used for HPLC analysis of (±)-2-bromomyristic acid in biological samples.

Time (min)	Amount of acetonitrile (%)	Amount of water (%)
0–14	20	80
16	30	70
17	40	60
19–35	50	50
37	40	60
38	30	70
40	20	80

regression analysis of the natural logarithms of the concentration and time values in the terminal phase. The elimination half-life ($\beta t_{1/2}$) was calculated from $0.693\lambda z^{-1}$. Blood clearance (CL) was calculated from the equation CL = intravenous dose/intravenous AUC, where the intravenous AUC was the value derived from the computer calculation for the area under the blood concentration–time curve. The brain/blood ratio for AZT was compared by use of a multiple-comparison test of mean values and also from AUC_{brain}/AUC_{blood}.

Results and Discussion

Concentrations of the test compounds in whole blood were used to calculate pharmacokinetic parameters. Pharmacokinetic parameters for **1** and **3** after doses of **1** and **3**, respectively, are presented in Table 3. These data show that $t_{1/2\alpha}$ (distribution, or alpha-phase, half-life) = 4·2 min and $t_{1/2\beta}$ = 428·5 min for the prodrug **3**, compared with $t_{1/2\alpha}$ = 4·4 min and $t_{1/2\beta}$ = 112·5 min for **1**. The short distribution half-life of **3** indicates that early blood concentrations are a crucial determinant of pharmacokinetic constants for the prodrug. Because of the high lipophilicity of **3**, its rapid in-vivo clearance from blood is thought to be attributable to its sequestration by lipoidal tissues such as liver and fat. The high initial blood levels after injection of **1** decreased rapidly, resulting in longer mean residence times (MRT) for **3** (379 min) than for **1** (156 min).

In Table 4 the pharmacokinetic parameters of the prodrug **3** and one of its metabolites (**1**) after a dose of **3** are compared with the pharmacokinetics of **1** after a dose of **1**. This critical comparison of the pharmacokinetic parameters for **1** from the two dosage forms (**1** and **3**) clearly shows that both brain and liver experience elevated levels of the therapeutic drug (**1**) after dosing with the prodrug (**3**).

Table 3. Parameters obtained from two-compartment modelling of the blood-clearance curves for equimolar doses of (±)-3′-azido-2′,3′-dideoxy-5′-*O*-(2-bromomyristoyl)thymidine and 3′-azido-2′,3′-dideoxythymidine (AZT) in the Balb/c mice.

Parameter*	(±)-3′-Azido-2′,3′-dideoxy-5′-*O*-(2-bromomyristoyl) thymidine	3′-Azido-2′,3′-dideoxythymidine
AUC (μmol g^{-1} min)	17·3 ± 4·7	29·1 ± 2·9
AUC(AZT) (μmol g^{-1} min)	12·3 ± 0·8	29·1 ± 2·9
$t_{1/2\alpha}$ (min)	4·2	4·4
$t_{1/2\beta}$ (min)	428·5	112·5
C_{max} (μmol g^{-1})	1·1 ± 0·1	0·4 ± 0·1
MRT (min)	379·0	155·9
CL (mL min^{-1} kg^{-1})	17·6 ± 4·8	10·5 ± 1·1
V_{SS} (mL)	183·3	44·9

* Calculated using the WinNonlin program.

Table 4. Selected pharmacokinetic parameters for (±)-3′-azido-2′,3′-dideoxy-5′-*O*-(2-bromomyristoyl)thymidine (**3**) and 3′-azido-2′,3′-dideoxythymidine (**1**, AZT) in mouse blood, brain and liver after administration of equimolar doses of the compounds.

Tissue	AZT or ester	C_{max} (μmol g^{-1})	AUC (μmol min g^{-1})
Blood	AZT (from **1**)	0·36 ± 0·07	29·1 ± 2·9
	Ester (from **3**)	1·12 ± 0·09	17·3 ± 4·7
	AZT (from **3**)	0·17 ± 0·02	12·3 ± 0·8
Brain	AZT (from **1**)	0·01 ± 0·001	1·4 ± 0·2
	Ester (from **3**)	ND	ND
	AZT (from **3**)	0·03 ± 0·002	2·8 ± 0·5
Liver	AZT (from **1**)	0·81 ± 0·14	12·7 ± 2·7
	Ester (from **3**)	2·48 ± 0·03	26·2 ± 8·1
	AZT (from **3**)	1·16 ± 0·28	42·5 ± 4·1

C_{max}, peak or maximum concentration. AUC, area under the curve of blood concentration against time extrapolated to infinity. ND = not detectable.

The blood level data for **1** and **3** after intravenous injection of **3** are presented in Figure 2 and Tables 5 and 6. Kawaguchi et al (1990, 1991) have reported that the plasma concentrations of the caproate and stearate esters of AZT were below the detection limit after intraperitoneal administration to mice. Several 5′-*O*-esters of AZT, such as AZT acetate, AZT decanoate and AZT stearate, could also not be detected in rat blood after intravenous administration (Kawaguchi et al 1990, 1991). This might be attributable to their rapid absorption into lipoidal tissues, because fatty tissues can act as reservoirs for the prodrugs. In contrast, the 5′-*O*-(2-bromomyristoyl) ester of AZT (**3**) was readily

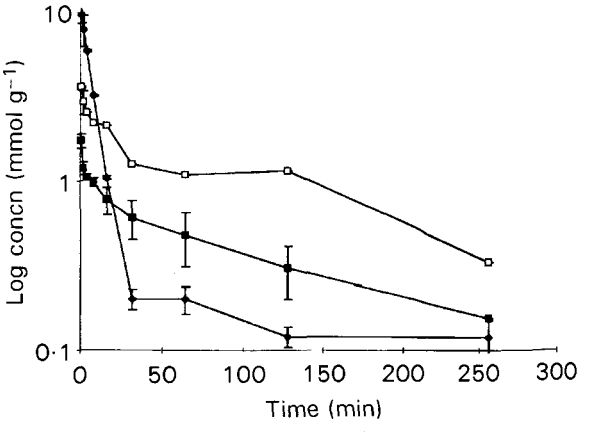

Figure 2. Concentrations (μmol g^{-1}) of AZT (**1**, ■) and prodrug (**3**, ◆) in blood of mice after intravenous tail-vein injection of **3** (169·8 mg kg^{-1}), and concentrations of **1** (□) after intravenous tail-vein injection of an equimolar dose (81·5 mg kg^{-1}) of **1**. Data are means ± s.e.m. (n = 3).

Table 5. Concentrations (μmol g^{-1}) of 3′-azido-2′,3′-dideoxythymidine (AZT, **1**) in liver, brain and blood of mice after intravenous tail-vein-injection of (±)-3′-azido-2′,3′-dideoxy-5′-*O*-(2-bromomyristoyl)thymidine (**3**; 169·8 mg kg^{-1}).

Time after injection (min)	Liver	Brain	Blood	Brain/blood ratio
1	1·11 ± 0·28	0·025 ± 0·002	0·17 ± 0·02	0·15
2	0·10 ± 0·05	0·021 ± 0·005	0·12 ± 0·01	0·18
4	0·57 ± 0·05	0·019 ± 0·004	0·11 ± 0·01	0·17
8	0·53 ± 0·03	0·015 ± 0·001	0·098 ± 0·001	0·15
16	0·31 ± 0·03	0·012 ± 0·002	0·08 ± 0·01	0·15
32	0·21 ± 0·03	0·010 ± 0·002	0·06 ± 0·02	0·17
64	0·21 ± 0·02	0·006 ± 0·001	0·05 ± 0·02	0·12
128	0·12 ± 0·00	0·005 ± 0·000	0·03 ± 0·01	0·17
256	0·02 ± 0·00	0·004 ± 0·001	0·02 ± 0·00	0·20

Data are means ± s.e.m. (n = 3).

Table 6. Concentrations (μmol g^{-1}) of 3′-azido-2′,3′-dideoxythymidine (AZT, **1**) in liver, brain and blood of mice after intravenous tail-vein-injection of the compound (81·5 mg kg^{-1}).

Time after injection (min)	Liver	Brain	Blood	Brain/blood ratio
1	0·26 ± 0·01	0·01 ± 0·00	0·36 ± 0·00	0·03
2	0·81 ± 0·14	0·016 ± 0·005	0·29 ± 0·05	0·06
4	0·24 ± 0·02	0·013 ± 0·002	0·25 ± 0·00	0·05
8	0·25 ± 0·01	0·014 ± 0·001	0·22 ± 0·00	0·06
16	0·18 ± 0·00	0·015 ± 0·000	0·21 ± 0·00	0·07
32	0·09 ± 0·01	0·008 ± 0·001	0·13 ± 0·00	0·06
64	0·05 ± 0·01	0·006 ± 0·000	0·11 ± 0·00	0·06
128	0·03 ± 0·00	0·003 ± 0·000	0·11 ± 0·00	0·03
256	0·03 ± 0·00	0·003 ± 0·000	0·03 ± 0·00	0·10

Data are means ± s.e.m. (n = 3).

detected in mouse blood in the current experiment and so other factors such as stability of the 5′-*O*-ester in blood must play a major role in the persistence of these nucleoside esters in the blood. Although high lipophilicity might cause accumulation of lipophilic esters in peripheral fatty tissues, the equilibrium between the blood and these tissues will be an important determinant of pharmacokinetic properties in the case of stable esters such as **3**.

A significant fraction of **3** was rapidly hydrolysed, as demonstrated by the presence of **1** (0·17 μmol g^{-1}) in blood within 1 min of injection. Most of the dose of **3**, however, seemed to have been distributed to tissues, because only 11·7% of the ester was present in blood within a minute of injection. The presence of **3** in blood after 480 min indicates that the compound undergoes equilibrium-based redistribution between peripheral tissues and blood for a prolonged period. Data are presented in Figure 2.

AZT (**1**) was readily detected and quantified in blood, brain and liver after intravenous injection of **3**. The blood AUC for **1**, as a metabolite of **3** (12·3 ± 2·9 μmol min g^{-1}) was less than when an equimolar dose of **1** itself was injected (29·1 ± 2·9 μmol min g^{-1}). Lower concentrations of **1** were observed in blood at all times after dosing with **3** than after administration of AZT (e.g. 0·36 and 0·17 μmol g^{-1}, respectively, 1 min post-injection of equimolar doses of either **1** or **3**; Tables 5 and 6).

To treat hepatitis B more effectively, it would be desirable to direct a larger fraction of the dose of AZT to the liver. This was achieved by use of the prodrug (**3**). However, because esterification of the 5′-hydroxyl group might also prevent or slow the glucuronidation of AZT, any decrease in AZT glucuronidation could also lead to a substantial increase in the half-life of AZT, because in man 75% of a dose of AZT is metabolized by hepatic glucuronidation to form 3′-azido-2′,3′-dideoxy-5′-

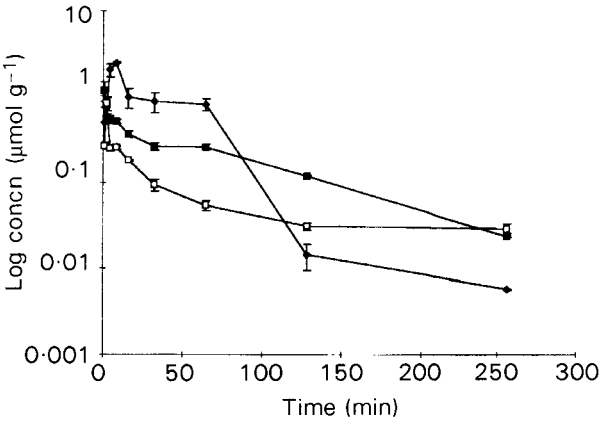

Figure 3. Concentrations (μmol g^{-1}) of AZT (**1**, ■) and (±)-3′-azido-2′,3′-dideoxy-5′-*O*-(2-bromomyristoyl)thymidine (**3**, ◆) in the livers of mice after intravenous tail-vein injection of **3** (169·8 mg kg^{-1}), and concentrations of **1** (□) after intravenous tail-vein injection of an equimolar dose (81·5 mg kg^{-1}) of **1**. Data are means ± s.e.m. (n = 3).

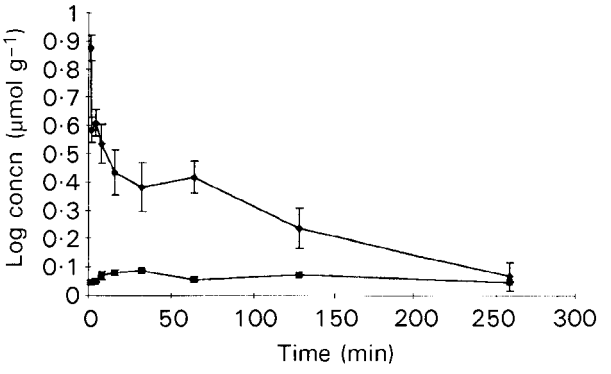

Figure 4. Concentrations of (±)-2-bromomyristic acid (**2**) in the livers of mice after intravenous tail-vein injection of **2** (93·7 mg kg^{-1}) (■), or after intravenous tail-vein injection of an equimolar dose (169·8 mg kg^{-1}) of **3** (◆). Data are means ± s.e.m. (n = 3).

O-glucuronyl thymidine, an inert metabolite (Moore et al 1995). An increase in the effective hepatic concentration of AZT would enable the use of lower doses of AZT to achieve the same therapeutic benefit. The results from this study (Figure 3) suggest that adequate delivery of AZT to the liver can be achieved with an appropriate ester derivative of AZT, such as **3**.

The prodrug (**3**) is present in the liver at higher concentrations than in blood (Figures 2 and 3). After 8 min, 29·6% of the dose of **3** was found in the liver. Further in-vivo studies are required to determine the proportion of the dose delivered to hepatic parenchymal cells rather than endothelial and Kupfer cells. Similarly, the hepatic concentration of **1** after injection of **3** was higher than after injection of **1** itself, which indicates that **3** also underwent higher hepatic extraction than **1** (Figure 3). This was confirmed by a comparative study which showed that **3** was accumulated to a concentration 4·5 times higher than that of **1** after doses of the respective compounds. The extensive distribution of the prodrug to the liver, particularly after very short times, is probably partly because of its high lipophilicity. The AUC for AZT (from **3**) in liver (AUC 42·5 ± 4·1 μmol min mL^{-1}) is larger than when AZT itself was injected (17·7 ± 2·7 μmol min mL^{-1}).

The metabolism of 2-bromomyristic acid (**2**) by the liver has not been investigated. The HPLC peak with a retention time of approximately 27 min was assigned to 2-bromomyristic acid on the basis of its coelution with authentic **2**. 2-Bromomyristic acid was not detectable in blood after administration by injection into the tail vein. Binding to plasma proteins such as albumin or lipoproteins (as triglycerides) (Mead & Howton 1960), absorption into blood cells (e.g. erythrocytes) and fatty tissues, and rapid metabolism might all contribute to its rapid clearance from the blood. 2-Bromomyristic acid was, however, detected in blood (0·1 μmol g^{-1}) for up to 2 min after injection of **3**.

The concentration of **2** in the liver after administration of **3** was greater than after dosing with **2** itself (Figure 4). This was attributed to higher relative extraction of **3** by the liver and then in-situ release by hydrolysis of **3**. It is possible that doses of **2** were rapidly degraded, either in the blood or liver, immediately upon injection.

In all studies no prodrug ester **3** was detected in brain samples and the levels of **1** in the brain were lower than in the blood and liver. There are several possible explanations for the apparent absence of **3** from brain:

Rapid egress of **3** occurred before hydrolysis could occur, because high lipophilicity would facilitate diffusion for both entry and egress; a rapid decline in blood levels would lead to equally rapid reductions in brain levels.

Compound **3** might have entered the brain and undergone rapid hydrolysis to liberate **1** before complete efflux, but this is unlikely because this process would afford the more polar and less lipophilic AZT, which should have been retained in the cell for a longer time.

Compound **3** might be too lipophilic or too large (MW 556·5 Da) for good permeation (Levin 1980). Because the extraction coefficient is related to the lipophilicity or *n*-octanol–water partition coefficient of a compound, which in turn is related to the ability of a compound to partition into phospholipoidal membranes, increased lipophilicity alone

does not ensure that a given prodrug will deliver higher concentrations of a parent compound to the CNS (Stella 1980).

Compound **3** might bind to circulating macromolecules, resulting in reduced extraction of this highly lipophilic compound by the brain. Support for this argument can be found in the work of Dishino et al (1983) who reported that the binding of a wide variety of non-ionic organic compounds to both bovine serum albumin and bovine haemoglobin seems to be linearly related to their *n*-octanol–water partition coefficients.

Although efflux of AZT from the brain via the organic-anion-transport system has a potential role in its concentration in the brain (Wang & Sawchuk 1995), no efflux transport system has been discovered for nucleoside ester prodrugs. It therefore seems that diffusion of **3** (owing to high lipophilicity) across the blood–brain barrier is inadequate to provide a measurable concentration of this prodrug in the brain and that regeneration to AZT in the brain is slow relative to its diffusion across the blood–brain barrier.

Time courses for the distribution of **1** to the brain after administration of **1** and **3** are shown in Figure 5. The maximum concentration of **1** in the brain after a dose of **3** was observed 1 min after injection, at the first time-point measured (Figure 5). The brain AUC for **1** derived from **3** ($2{\cdot}8 \pm 0{\cdot}5$ μmol min mL^{-1}) was greater than when **1** itself was administered ($1{\cdot}4 \pm 0{\cdot}02$ μmol min mL^{-1}). The concentration of **1** in the brain 1 min after dosing with **3** ($25{\cdot}69 \pm 2{\cdot}41$ nmol g^{-1}) was also higher than after dosing with **1** ($9{\cdot}84 \pm 0{\cdot}77$ nmol g^{-1}). These concentrations were higher than those previously obtained with the dihydropyridine carrier system coupled to nucleosides (Palomino et al 1989; Chu et al 1990) and glycosyl triester derivatives (Namane et al 1992). For example, Namane et al (1992) measured AZT concentrations of 1·5 and 4·9 nmol g^{-1} after administration of a glycosyl phosphotriester of AZT and of AZT, respectively.

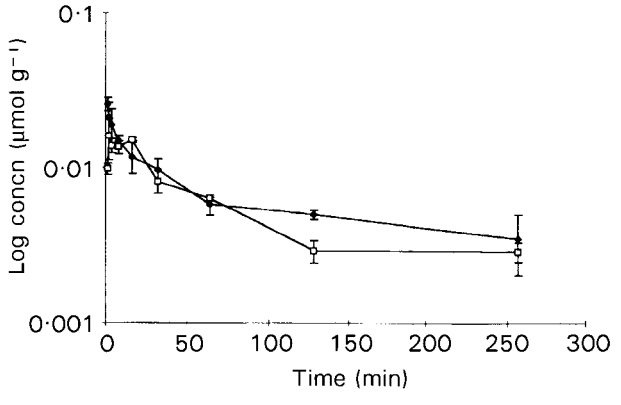

Figure 5. Concentrations of AZT in the brains of mice after intravenous tail-vein injection of equimolar doses of **3** (169·8 mg kg^{-1}, ◆) and **1** (81·5 mg kg^{-1}, □). Data are means ± s.e.m. (n = 3).

The relative brain exposure, r_e, to **1** (AZT) was calculated as $r_e = (AUC)_{PD \rightarrow P}/(AUC)_P = 2{\cdot}07$, where $(AUC)_{PD \rightarrow P}$ is the area under the brain AZT concentration–time curve after administration of the prodrug (PD, **3**), and $(AUC)_P$ is the same area obtained after administration of the parent (P, **1**) compound, AZT (Table 4). Favourable delivery of the parent drug to the brain after administration of the prodrug is indicated by $r_e > 1$. The relative brain exposure for AZT (2·07) indicates a significant increase in exposure to AZT after administration of prodrug. The r_e value clearly indicates that **1** has a longer residence time in the brain after administration of **3** than after administration of **1**, suggesting that **3** has a pharmacokinetic advantage over AZT. This analysis revealed that 1 min after dosing systemic administration of the prodrug resulted in 2·6 times more AZT in the brain than did an equimolar dose of AZT itself.

The concentrations of 2-bromomyristic acid (**2**) in brain were not significantly different after injection of either **2** or **3**—after 2 min the concentrations of **2** were 0·04 and 0·03 μmol g^{-1}, respectively. 2-Bromomyristic acid was not detectable at post-injection intervals longer than 2 min. The low concentration of **2** in the brain could be because of its binding to plasma proteins, rapid metabolism, rapid efflux, or diffusion into peripheral tissues.

Brain/blood concentration ratios for AZT in mice after administration of 50 mg kg^{-1} and 250 mg kg^{-1} have been reported to be dose-dependent, the ratios being higher after doses of 250 mg kg^{-1} (brain/serum = $0{\cdot}28 \pm 0{\cdot}64$) than after doses of 50 mg kg^{-1} (brain/serum = $0{\cdot}06 \pm 0{\cdot}03$) (Doshi et al 1989). The brain/blood ratio measured in the current study was $0{\cdot}057 \pm 0{\cdot}001$ after an intravenous bolus dose of 81·5 mg kg^{-1} of **1**. The highest brain/blood concentration ratio after dosing with **1** was 0·1 (after 256 min), whereas the brain/blood concentration ratio for AZT after administration of **3** was 0·2 at the same time post-dose (Tables 5 and 6). The $AUC_{brain/blood}$ ratios for AZT after dosing with prodrug (**3**) and AZT (**1**) were 0·23 and 0·05, respectively (Table 4). These data indicate that delivery of AZT to brain is significantly increased by use of the prodrug.

In conclusion, in mice the AZT prodrug **3** has the pharmacokinetic properties and brain and liver delivery characteristics required to reduce the toxicity and increase the efficacy of AZT-based

AIDS therapy. Delivery of the antifungal myristic acid **2** might be an added benefit to the use of **3** in treating opportunistic infections associated with the AIDS syndrome.

Acknowledgements
We are grateful to the Alberta Heritage Foundation for Medical Research for a studentship award (K. Parang) and to the Medical Research Council of Canada for financial support of this research.

References

Aggarwal, S. K., Gogu, S. R., Rangan, S. R. S., Agrawal, K. C. (1990) Synthesis and biological evaluation of prodrugs of zidovudine. J. Med. Chem. 33: 1505–1510

Chu, C. K., Bhadti, V. S., Doshi, K. J., Etse, E. T., Gallo, J. M., Boudinot, F. D., Schinazi, R. F. (1990) Brain targeting of anti-HIV nucleosides: synthesis and in vitro and in vivo studies of dihyropyridine derivatives of 3′-azido-2′,3′-dideoxyuridine and 3′-azido-3′-deoxythymidine. J. Med. Chem. 33: 2188–2192

Czernecki, S., Valery, J.-M. (1991) An efficient synthesis of 3′-azido-3′-deoxythymidine (AZT). Synthesis 239–240

Diamond, R. D. (1995) *Cryptococcus neoformans*. In: Mandell, G. L., Douglas, R. G., Bennett, J. E., Dolin, R. (eds) Principles and Practice of Infectious Diseases, 4th edn. Churchill Livingstone, New York, p. 2331

Dishino, D. D., Welch, M. J., Kiburn, M. R., Raichle, M. E. (1983) Relationship between lipophilicity and brain extraction of C-11-labeled radiopharmaceuticals. J. Nucl. Med. 24: 1030–1038

Doshi, K., Gallo, J., Boudinot, F., Schinazi, R., Chu, C. (1989) Comparative pharmacokinetics of 3′-azido-3′-deoxythymidine (AZT) and 3′-azido-2′,3′-deoxyuridine (AZddU) in mice. Drug Metab. Dispos. 17: 590–594

Kamijo, T., Harada, H., Iizuka, K. (1984) An improved and convenient synthesis of esters using 1,1′-carbonyldiimidazole and a reactive halide. Chem. Pharm. Bull. 32: 5044–5047

Kawaguchi, T., Ishikawa, K., Seki, T., Juni, K. (1990) Ester prodrugs of zidovudine. J. Pharm. Sci. 79: 531–533

Kawaguchi, T., Endoh, T., Seki, T., Juni, K. (1991) Plasma concentrations of zidovudine in rats via oral administration of its ester prodrugs. J. Pharm. Sci. 80: 404–405

Koenig, S., Gendelman, H. E., Orenstein, J. M., Dal Canto, M. C., Pezeshkpour, G. H., Yungbluth, M., Janotta, F., Aksamit, A., Martin, M. A., Fauci, A. S. (1986) Detection of AIDS virus in macrophages in brain tissue from AIDS patients with encephalopathy. Science 233: 1089–1093

Levin, V. A. (1980) Relationship of octanol/water partition coefficient and molecular weight to rat brain capillary permeability. J. Med. Chem. 23: 682–684

Mead, J. F., Howton, D. R. (1960) Transport, deposition and mobilization of fatty acids. In: Radioisotope Studies of Fatty Acid Metabolism. Pergamon Press, New York, Chapter II, pp 15–22

Moore, K. H. P., Raasch, R. H., Brouwer, K. L. R., Opheim, K., Cheeseman, S. H., Eyster, E., Lemon, S. M., Horst, C. M. (1995) Pharmacokinetics and bioavailability of zidovudine and its glucuronidated metabolite in patients with human immunodeficiency virus infection and hepatic disease (AIDS clinical trials group protocol 062). Antimicrob. Agents Chemother. 39: 2732–2737

Namane, A., Gouyette, C., Fillion, M.-P., Fillion, G., Huynh-Dinh, T. (1992) Improved brain delivery of AZT using a glycosyl phosphotriester prodrug. J. Med. Chem. 35: 3039–3044

Palomino, E., Kessel, D., Horwitz, J. P. (1989) A dihydropyridine carrier system for sustained delivery of 2′,3′-dideoxynucleosides to the brain. J. Med. Chem. 32: 622–625

Parang, K., Knaus, E. E., Wiebe, L. I., Sardari, S., Daneshtalab, M., Csizmadia, F. (1996) Synthesis and antifungal activities of myristic acid analogs. Arch. Pharm.-Pharm. Med. Chem. 329: 475–482

Pizzo, P. A. (1990) Pediatric AIDS: problems within patients. J. Infect. Dis. 161: 316-325

Stella, V. J. (1980) Prodrugs and site-specific drug delivery. J. Med. Chem. 23: 1275–1282

Wang, Y., Sawchuk, R. J. (1995) Zidovudine transport in the rabbit brain during intravenous and intracerebroventricular infusion. J. Pharm. Sci. 84: 871–876